Scaling law and flux pinning in polycrystalline $La_{1.85}Sr_{0.15}CuO_4$

D. P. Hampshire
The Applied Superconductivity Center, University of Wisconsin, Madison, Wisconsin 53706

J. A. S. Ikeda and Y.-M. Chiang
Department of Materials Science and Engineering, Massachusetts Institute of Technology, Cambridge, Massachusetts 02139

(Received 24 April 1989; revised manuscript received 12 July 1989)

The transport critical current density (J_{ct}) of two hot-pressed bulk polycrystalline $La_{1.85}Sr_{0.15}CuO_4$ superconducting samples has been measured over the temperature range 2 K to T_c in magnetic fields up to 27 T. It is demonstrated that these data have a separable variable form $F_p = J_{ct}B = \alpha(D)B_{c2}^{2.4}(T)b$ [where $\alpha(D)$ is a constant and $b = B/B_{c2}(T)$], in agreement with the Fietz-Webb scaling law. This is strong evidence that in high magnetic fields, flux pinning is the mechanism that determines the critical current density. The authors suggest that the dissipative state is described by flux flow along the regions of weak flux pinning at the grain boundaries.

I. INTRODUCTION

Despite the enormous effort towards understanding high-T_c superconductors, the transport critical current density (J_{ct}) of bulk polycrystalline samples in high magnetic fields is still low. In this article, the critical current density is presented over the temperature range from 2 K to T_c in magnetic fields up to 27 T of two sintered samples of hot-pressed polycrystalline $La_{1.85}Sr_{0.15}CuO_4$. With these data we derive the functional form of the critical current density. This functional form allows us to characterize the mechanisms which determine J_{ct}. By identifying and understanding these mechanisms, we may be able to increase the critical current density of these materials.

A simple explanation of the low J_{ct} in polycrystalline samples has been developed in the community within the framework of weak links. It is well established that single crystals and thin films can support large critical current densities.[1-3] Hence it is argued that polycrystalline samples consist of regions of high critical current, completely separated from each other by weak links.[4-6] These weak links can support only small critical current densities in high magnetic fields.

The location and nature of the weak links is not yet ascertained. There is strong evidence that grain boundaries are weak links and additional evidence that there may be intragranular weak links as well.[2,4-8]

It has been suggested that the superconductivity in single crystals is intrinsically two dimensional. Within this framework the single crystals contain alternating superconducting and insulating layers.[9] This layered structure occurs either because of the intrinsic crystal structure or because of twin boundaries.[10,11] Alternatively it has been suggested that although the single crystals are three dimensional, consistent with a Bardeen-Cooper-Schrieffer formalism,[12,13] the coherence length is sufficiently short to ensure that the grain boundaries are not superconducting.[8,14] Both of these descriptions have a common explanation for the low J_{ct} in polycrystalline samples: Most of the grain boundary area is not superconducting in high magnetic fields.[15-17] Therefore the transport critical current is very low indeed.

The approach which considers the grains as poorly coupled has formally been described by modeling the grain boundaries as Josephson junctions. Several authors have proposed that the fraction of grain boundary area that is active is about one part in 10^3 in zero field.[8,14,17] In high fields a second mechanism is invoked. It is assumed that a superconducting percolative path which has a high B_{c2} but constitutes an even smaller fraction of the grain boundary area supports the supercurrent.

The extensive electromagnetic data in the literature demonstrates that weak links occur in $BaPb_{1-x}Bi_xO_3$, $La_{1.85}Sr_{0.15}CuO_4$, and $RBa_2Cu_3O_7$ (where R is a rare-earth element). In these oxide superconductors, a comparison of single-crystal thin films with bulk polycrystalline samples shows similar features. The critical current density in thin films is a decreasing function of magnetic field over the range $0 \ll B < B_{c2}(T)$ and is typically three orders of magnitude higher than that found in bulk polycrystalline samples.[1,18,19] In many bulk polycrystalline samples, prepared using a number of different fabrication techniques, the critical current density is field independent over the range $0 \ll B < B_{c2}(T)$.[20-22] The prevalence of weak-link behavior suggests that the results presented in this work on La-Sr-Cu-O are characteristic of many bulk polycrystalline samples from the class of high-T_c oxide superconductors.

In this work a very different description for the weak links is proposed. The hypothesis is developed that the grains are essentially fully coupled, and the poor flux pinning properties of the grain boundaries are responsible for the low values of J_{ct}. This is analogous to the transport current density of well-ordered single crystals of low-T_c metallic superconductors.[23] Although the depair-

ing current density (J_D) is very high, a voltage is developed at very low current densities because of the very weak pinning that is present.

A milestone in our understanding of flux pinning was the work by Fietz and Webb[24] which demonstrated that the volume pinning force ($F_p = J_{ct}B$) obeyed a scaling law of the form $F_p = \alpha(D)B_{c2}^n(T)f(b)$ [where $\alpha(D)$ is determined solely by the microstructure, $B_{c2}(T)$ is the upper critical field, and $f(b)$ is a function only of the reduced field $b = B/B_{c2}(T)$]. The volume pinning force of a great number of alloys, intermetallic compounds, and Chevrel phase superconductors is described by this scaling law.[25–28] Many different expressions have been derived theoretically[29,30] for the volume pinning force, all of which are of the separable variable form, as required by this law. Historically, in addition to the scaling law, there are two other sources of evidence which led to the general acceptance of flux pinning as the mechanism which determines the critical current density. First, decoration measurements showed that fluxons were preferentially located on defects and grain boundaries.[31,32] Second, it was found that by increasing the density of pinning sites the critical current density increased.[33]

A number of authors have considered whether the high *intragranular* current densities that have been found, obey the Fietz-Webb scaling law.[14] In this work we focus on the *intergranular* current density. By measuring the transport critical current density as a function of field and temperature in polycrystalline samples we determine whether the volume pinning force obeys the Fietz-Webb scaling law.

There are significant problems in an investigation of whether the volume pinning force of the high-T_c oxides obeys the Fietz-Webb scaling law. In many of these materials the B_{c2} values are well above the level of dc magnetic field available in even the best high-field laboratories.[34] In addition because of the highly anisotropic expansion coefficients, bulk materials of the $R\,Ba_2Cu_3O_{7-y}$ series are susceptible to microcracking when cooling from the sintering temperature (-900 K) to a cryogenic temperature for testing. Microcracking prevents an accurate measurement of the area over which the current flows. In light of this we have chosen to investigate two hot-pressed La-Sr-Cu-O samples. The anisotropy in the expansion coefficient of La-Sr-Cu-O are such that in these fine-grain-size samples we can avoid significant microcracking.[35] In addition, B_{c2} is sufficiently low that it can be measured directly.[36,37]

II. SAMPLE PREPARATION

A freeze-dried-acetate process similar to that described by Johnson *et al.*[38] was used to prepare the constituent powders of composition $La_{1.85}Sr_{0.15}CuO_4$, La, Sr, and Cu acetates were assayed in the appropriate proportions, dissolved into distilled water, and thoroughly mixed. The solution was then sprayed into liquid nitrogen, and the frozen particulates were freeze dried in a cycle whereby the temperature of the material was slowly raised to 100 °C under vacuum over a period of five days. After subsequent pyrolysis at 850 °C, equiaxed powders (diameter 0.1–0.2 μm) of the K_2NiF_4 structure were produced. These powders were single phase as determined by x-ray diffraction. The calcined powder was then uniaxially pressed at 275 MPa into pellets (20 mm diam × 5 mm thick) which were subsequently tightly sealed in gold foil and hot pressed in flowing oxygen at 900 °C for 3.5 h at a pressure of 33 MPa. After hot pressing, the sintered pellet was 95–100 % dense and had an average grain size of about 1 μm.

The pellet was sectioned to produce bars of dimensions $2 \times 7 \times 2$ mm^3. Two different samples were then produced by subjecting the bars to a grain growth anneal (1000 °C in flowing oxygen) for 1 and 10 h. This produced samples with different average grain size of ~ 1 (sample A) and ~ 3 μm (sample B), respectively. Both samples were subsequently annealed at 700 °C for 66 h in flowing oxygen to restore their oxygen stoichiometry. Figures 1(a) and 1(b) are micrographs showing the grain size and morphology of the two samples.

The advantages of this preparation route are that it produces an excellent homogeneity, accurate control of cation stoichiometry, and a narrow distribution of fine grain size.

III. EXPERIMENTAL RESULTS

The samples were prepared for electrical measurements by sputter depositing four thin (0.2 μm) gold contact pads of area $\sim 2 \times 2$ mm^2 onto the samples. These contacts have sufficiently low surface resistivities to ensure negligible heating during measurement.[39]

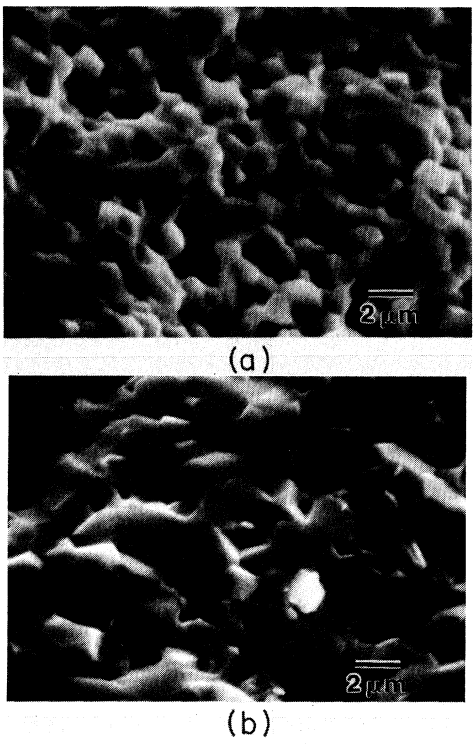

FIG. 1. Secondary electron images of the samples used in this work. (a) ~ 1 μm grain size (sample A); (b) ~ 3 μm grain size (sample B).

A. Resistivity

In Fig. 2 the resistivity is plotted as a function of temperature. Both samples attained zero resistivity at 36 K and had δT_c (25–75%)=2 K. The normal-state resistivity values are 1.4 and 0.6 mΩ cm just above T_c for samples A and B, respectively. In single crystals at 40 K it has been found that the resistivity is 20 and 1 mΩ cm, parallel and orthogonal to the c axis, respectively.[36] Our polycrystalline samples thus have a very low resistivity in comparison to a crystallographically averaged value of the single-crystal data. This suggests that we have achieved very good homogeneity and stoichiometry in these samples and low grain boundary resistivity.

B. Critical current density

Standard four-terminal voltage-current data were generated as a function of field and temperature. The data at 2 and 4.2 K were obtained by directly immersing the sample in liquid helium, and the temperature was regulated using vapor pressure control. At temperatures above 4.2 K, a variable temperature insert was used. This insert isolated the sample from the helium bath. In zero field the temperature was fixed at that required, using a calibrated carbon glass thermometer as a standard. A field-independent strontium titanate capacitance control thermometer was then used in closed loop with a heater to keep the temperature constant when the magnetic field was applied. The uncertainty in temperature for these data is about 4%.

In Figs. 3 and 4, the critical current density as a function of field and temperature is presented. The electric field criterion used to define J_{ct} was 10 μV cm^{-1}. This criterion was chosen as a compromise between a sufficiently low value to reduce heating problems and yet a sufficiently high value to achieve good signal to noise. It is of note that these E-J transitions are quite broad. By defining J_{ct} as the first detectable voltage (2 μV cm^{-1}), the values quoted would typically be reduced by 15%. This should be compared with a typical reduction of 10% for Nb_3Sn materials of high J_{ct} and 4% for NbTi materials of high J_{ct} for the same criteria.

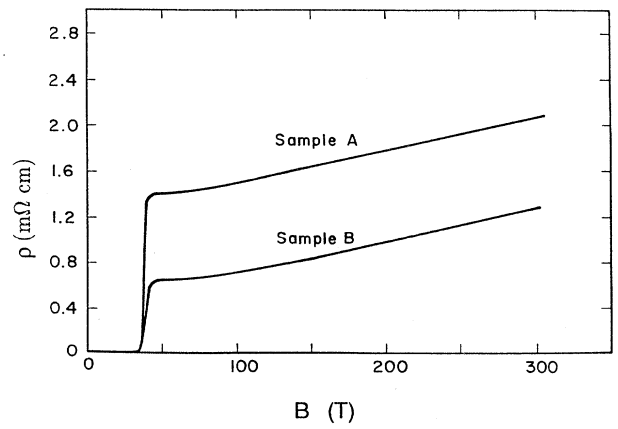

FIG. 2. The resistivity as a function of temperature for samples A and B.

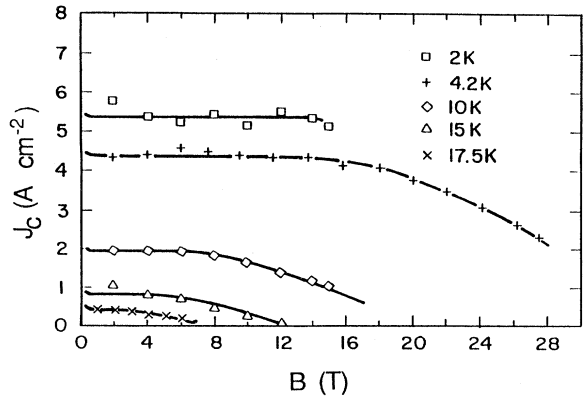

FIG. 3. The critical current density as a function of field and temperature for sample A.

Figures 3 and 4 demonstrate that the critical current density is largely independent of field at intermediate magnetic fields and increases as the temperature decreases. These characteristics have been observed before in many $R Ba_2Cu_3O_7$ systems.[21,22] However unlike the $R Ba_2Cu_3O_7$ systems at 4.2 K, at high fields (above 25 T), J_{ct} decreases strongly. The analysis below suggests that the reduction in J_{ct} at high fields can be associated with the applied field being equal to $B_{c2}(T)$ for some of the grains in the sample. Direct measurements of $B_{c2}(T)$ allows us to evaluate whether or not F_p obeys the Fietz-Webb scaling law.

C. Dissipation

Considerable effort has been directed at understanding the dissipative mechanisms which operate in superconductors during flux flow. In general, experimental and theoretical work are compared by considering the differential resistivity. In light of this, we have calculated the average differential resistivity above J_{ct} over the range 10 μV cm^{-1}–20 μV cm^{-1} (denoted ρ_I) for the two samples. In Figs. 5 and 6, ρ_I is presented as a function of field and temperature. The uncertainty in ρ_I is typically 20%. For clarity, a single characteristic at low, inter-

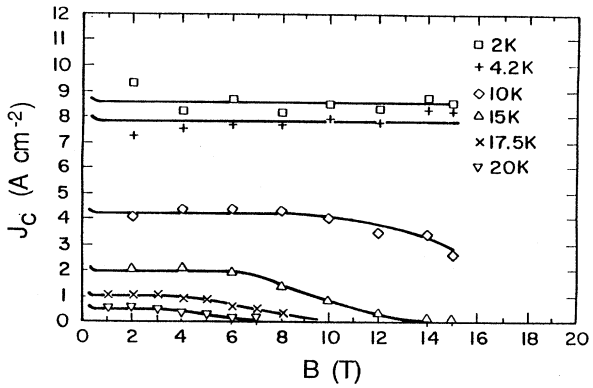

FIG. 4. The critical current density as a function of field and temperature for sample B.

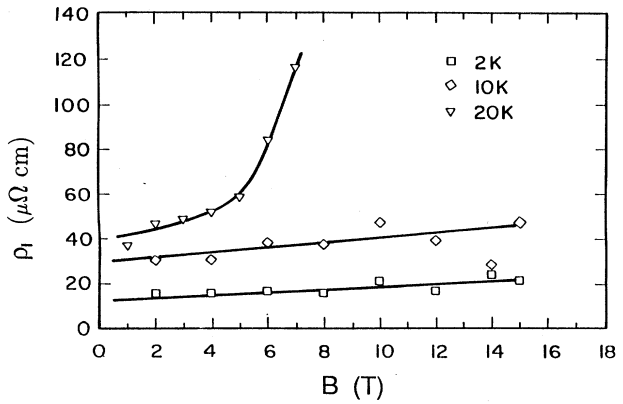

FIG. 5. The differential resistivity (ρ_I) above J_{ct} determined in the range 10–20 μV cm^{-1} as a function of field and temperature for sample A.

mediate, and high temperature for each sample are presented. These data demonstrate the general trends in ρ_I namely that it is an increasing function of field and temperature, and an extrapolation of ρ_I to zero magnetic field is nonzero.

IV. ANALYSIS OF DATA

A. Universal scaling laws

When the functional form of the volume pinning force is of a Fietz-Webb[24] separable variable form, where

$$F_p = \alpha(D) B_{c2}^n(T) f(b) , \quad (1)$$

this provides strong evidence that flux pinning is the mechanism which determines J_{ct}.

In all the experimental comparisons with this law it has been assumed that current flows over the entire cross-sectional area of the sample. If this law is tested in a field and temperature range over which this assumption is not valid, the field and temperature dependence of the active area over which current flows must also be incorporated into the expression for F_p. In order to avoid the complications of this additional term, in an anisotropic material this law must be tested over a field and temperature range below B_{c2} for all possible orientations of the grains with respect to the applied field. By restricting the field-temperature range to ensure all the grains are superconducting, it is not necessary to incorporate a correction to the sample cross-sectional area to account for some of the grains being in the normal state.

Measurements on single crystals of La-Sr-Cu-O demonstrate that when the applied field is parallel to the c axis, $B_{c2}(T)$ is 12 T at 4.2 K. For the orientation $\mathbf{B} \perp \mathbf{c}$, B_{c2} is 60 T—about five times larger.[36] Hence it is not unreasonable to attribute the decrease in J_{ct} at high fields shown in Figs. 2 and 3 to the applied field driving into the normal state a significant number of grains oriented such that their c axes are approximately parallel to the applied field. As such, we shall restrict our analysis to the intermediate fields (i.e., <18 T at 4.2 K) where at a given temperature J_{ct} is essentially independent of field and the single-crystal data suggest that essentially all the grains are superconducting.

B. Volume pinning force

In Figs. 7 and 8 the volume pinning force is presented as a function of field and temperature for the two samples. F_p has been calculated using the data in Figs. 3 and 4 and the definition $F_p = J_{ct} B$. In the intermediate field range over which J_{ct} is constant, the pinning force is a linear function of magnetic field. More importantly it can also be seen that at higher temperatures, F_p has a peak at a field value that is approximately half of the field value for which F_p extrapolates to zero.

C. Upper critical field

In order to test whether the volume pinning force obeys the Fietz-Webb scaling law given by Eq. (1), it is necessary to determine an appropriate value for $B_{c2}(T)$ for our polycrystalline samples. Unlike the isotropic superconductors which have a unique value of $B_{c2}(T)$, the

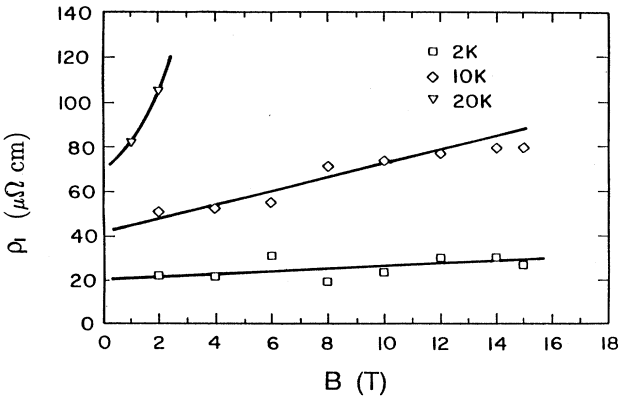

FIG. 6. The differential resistivity (ρ_I) above J_{ct} determined in the range 10–20 μV cm^{-1} as a function of field and temperature for sample B.

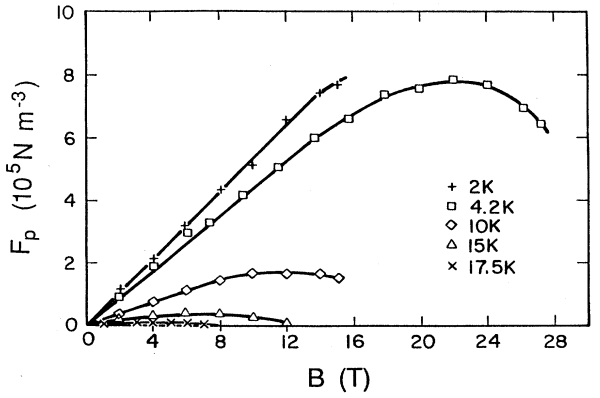

FIG. 7. The volume pinning force as a function of field and temperature for sample A.

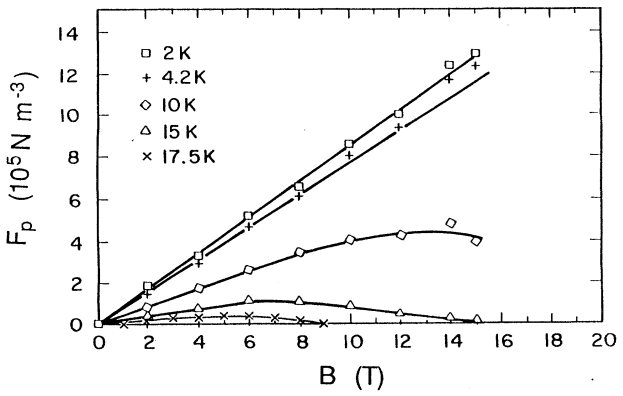

FIG. 8. The volume pinning force as a function of field and temperature for sample *B*.

anisotropic high-T_c oxides have an intrinsic distribution of $B_{c2}(T)$ values. *A priori* it is not clear which value from the distribution of $B_{c2}(T)$ is the appropriate value.

In Fig. 9, $B_{c2}(T)$ is plotted as a function of temperature using three different criteria. The lowest curve is defined by the field which decreases the constant value of J_{ct} found at intermediate fields (i.e., J_{ct}^*), by 10%. The middle curve is defined by the field at which J_{ct}^* is decreased by 50%. The upper curve is defined by the field at which J_{ct} (more strictly F_p) extrapolates to zero. At higher temperatures $B_{c2}(T)$ is defined by extrapolating directly the high-field volume pinning force to zero. It is clear from the pinning force curves that the peak in the pinning force occurs at half the value that is found for B_{c2} defined by the extrapolation. At lower temperatures,

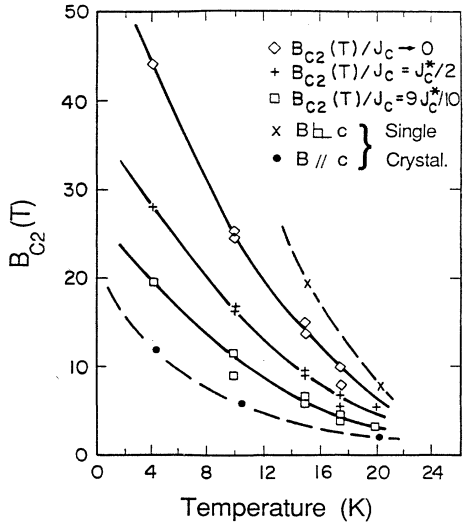

FIG. 9. The upper critical field defined using three different criteria (diamond the field at which $J_{ct} \to 0$; cross, the field at which $J_{ct} = J_{ct}^*/2$; square, the field at which $J_{ct} = 9J_{ct}^*/10$) as a function of temperature. Also shown for comparison are the upper critical field data of a single crystal, determined by resistive measurements by Hidaka *et al.* (Ref. 36) for the applied field parallel and orthogonal to the *c* axis.

we have defined the extrapolated value of $B_{c2}(T)$ as twice the value of field for which the volume pinning force is at its peak.

The most striking feature of Fig. 9 is the positive curvature of $B_{c2}(T)$. This has been observed previously in oxide superconductors[40,41] but is not observed in metallic low-T_c superconductors. A discussion of this curvature is provided in Sec. V.

D. Functional form of J_{ct} and F_p

Over the intermediate field range J_{ct} is independent of field and can be characterized by an equation of the form:

$$J_{ct}(B,T) = J_{ct}^*(T) , \tag{2}$$

where $J_{ct}^*(T)$ is a function only of temperature. In Fig. 10 the form of $J_{ct}^*(T)$ is explicitly determined by plotting $\log_{10}[J_{ct}^*(T)]$ versus $\log_{10}[B_{c2}(T)]$ using the three different criteria for $B_{c2}(T)$. In sections *X*, *Y*, and *Z* of this figure, $B_{c2}(T)$ is defined at $9J_{ct}^*/10, J_{ct}^*/2$ and $J_{ct} \to 0$, respectively. From this figure it can be seen that for both samples

$$J_{ct}(B,T) = \alpha B_{c2}^{1.4}(T) , \tag{3}$$

where the constant prefactor α is dependent on the criterion used and the sample. In Table I the values of α are presented for the two samples for each of the different criteria for $B_{c2}(T)$.

We now evaluate how sensitive Eq. (3) is to the electric field criterion that is used to define the critical current. A similar analysis to that is shown in Fig. 10 is shown in Fig. 11. However in Fig. 11, the criterion for B_{c2} is fixed (i.e., the field at which $J_{ct} = J_{ct}^*/2$) and the data are calculated using three different electric field criteria. Figure 11 demonstrates that the index for $B_{c2}(T)$ in Eq. (3) varies between 1.3 and 1.45 depending on the electric field criterion and the sample.

In summary the functional form of Eq. (3) is only weakly dependent on the criterion that is used to define B_{c2} or the electric field criterion that is used to define J_{ct}.

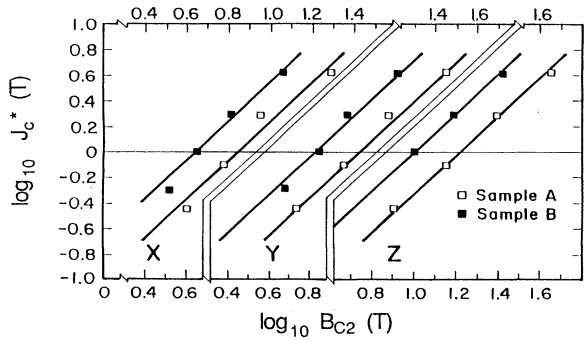

FIG. 10. A Log_{10}-Log_{10} plot of the critical current density in the intermediate field range (J_{ct}^*) vs the upper critical field for both samples. In sections *X*, *Y*, and *Z*, B_{c2} is defined by the field at which $J_{ct} = 9J_{ct}^*/10, J_{ct} = J_{ct}^*/2$, and $J_{ct} \to 0$, respectively.

TABLE I. The parameter α (10^{-2} $A\,cm^{-2}\,T^{-1.4}$) for the two samples calculated from $\alpha = J_c^*(T)/B_{c2}^{1.4}(T)$ [Eq. (3)] by defining J_{ct} at 10 $\mu V\,cm^{-1}$ and using the three different criteria for B_{c2} (X, Y, and Z are such that B_{c2} is defined by the field at which $J_{ct} = 9J_{ct}^*/10$, $J_{ct} = J_{ct}^*/2$, and $J_{ct} \to 0$, respectively). Also shown is the average grain size of the two samples.

	X	Y	Z	Grain size
Sample A	6.09	3.25	1.80	~ 1 μm
Sample B	11.76	6.72	3.72	~ 3 μm

Hence an expression for the volume pinning force is given in the form:

$$\mathbf{F}_p(B,T) = \mathbf{J}_{ct}(B,T) \times \mathbf{B} = \alpha B_{c2}^n(T) b \ , \tag{4}$$

where $n = 2.4 \pm 0.3$ and b is the reduced field. Equation (4) demonstrates a most important result: The volume pinning force of both of the La-Sr-Cu-O samples investigated in this work obeys the Fietz-Webb scaling law.

V. DISCUSSION

A. The upper critical field B_{c2}

In Fig. 9, B_{c2} has been plotted using three different criteria. The values of B_{c2} that have been obtained can be compared with single-crystal data that are also shown in this figure. This comparison allows us to derive a physical interpretation for the lower, middle, and upper curves in Fig. 9. These curves can be associated with the B_{c2} values of those grains oriented such that they have a low B_{c2} (i.e., $\mathbf{B} \| \mathbf{c}$), an average value of the distribution of B_{c2}, and a B_{c2} value for those grains oriented to give the highest value of B_{c2} (i.e., $\mathbf{B} \perp \mathbf{c}$), respectively.

The convex functional form for the temperature dependence of $B_{c2}(T)$ shown in Fig. 9 is not found in homogeneous low-T_c metallic superconductors.[42] However in inhomogeneous systems where one can expect a distribution in the fundamental parameters, a convex functional form for $B_{c2}(T)$ is found close to T_c.[43] In the La-Sr-Cu-O system however, even the single crystals show a convex behavior for $B_{c2}(T)$.[36] Hence one can interpret the $B_{c2}(T)$ data shown in Fig. 9 as suggesting that both the single crystal of Hidaka *et al.*[36] and our samples are to some degree inhomogeneous. In our polycrystalline samples the inhomogeneity may be associated with the strontium segregation to the grain boundaries. It is clear that the functional form of $B_{cs}(T)$ we measure (Fig. 9) is determined by the properties of the superconducting regions through which flux is moving at J_{ct}. As such, the convex form of $B_{c2}(T)$ is consistent with the suggestion in Sec. VI that there is a variation in critical parameters at the grain boundaries and at J_{ct} flux flows along the grain boundaries. It is of note that a similar convex form for $B_{c2}(T)$ to that shown in Fig. 9 has been found in the $YBa_2Cu_3O_7$ system and has been interpreted in terms of an irreversibility line.[44] At present there is no formalism that incorporates the physical processes which underpin the interpretation of the data in Fig. 9 as an irreversibility line into the Fietz-Webb framework. Alternatively it remains possible that the convex functional form of $B_{c2}(T)$ may be an intrinsic property.

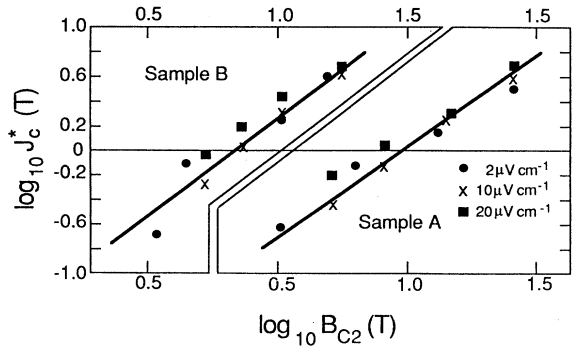

FIG. 11. A Log_{10}-Log_{10} plot of the critical current density in the intermediate field range vs the upper critical field at three different electric field criteria. B_{c2} is defined as the field at which $J_{ct} = J_{ct}^*/2$.

B. Differential resistivity

Only in the most simple systems has the differential resistivity above J_{ct} been derived theoretically. These calculations consider the synchronous motion of the entire flux line lattice across a superconductor with no pinning.[23,45–48] For a nonparamagnetically limited superconductor of high κ it has been shown that[47]:

$$\rho_f = \lim_{J_{ct} \to 0} (\partial E/\partial J)_{J > J_{ct}} = \rho_N g(T) B/B_{c2}(T) \ , \tag{5}$$

where ρ_f is known as the flux-flow resistivity and $g(T)$ is in general a complex function of temperature, where, for example, in the dirty limit[48] $g(T)_{T \to T_c} = 0.9(1 - T/T_c)^{1/2}(0.18l/\xi_0)$ (l, electronic mean free path; ξ_0, zero-temperature coherence length).

In the high-T_c superconductors the intrinsic dissipative mechanisms operating during flux flow have not been identified. In addition we argue below that dissipation occurs primarily at the grain boundaries, and hence expect a large-grain boundary-scattering contribution to the dissipation. We do note that two trends observed in both samples, namely that $(\partial E/\partial J)_{J > J_{ct}}$ increases as the field and the temperature increases, are the same trends predicted in Eq. (5) and found experimentally in superconductors both with[27,28,49] and without[45–48] pinning. The most significant difference between $(\partial E/\partial J)_{J > J_{ct}}$ in systems with pinning (i.e., ρ_I) and ρ_f is the difference in the magnitude of these two parameters. It has been shown that in high-J_{ct} materials ρ_I can be as small as $10^{-5}\rho_n$ (the normal-state resistivity above T_c).[49] In this work we have found that ρ_I is about $2 \times 10^{-2}\rho_n$. Considering Eq. (5), the magnitude of ρ_I suggests that about 2% of the total flux that is penetrating the sample is in motion at J_c. However, since our understanding of flux flow in the systems with pinning is so rudimentary, we have at present no explanation for the functional form of $(\partial E/\partial J)_{J > J_{ct}}$ that we have found experimentally.

C. The microstructural dependence of α

In a Fietz-Webb analysis the prefactor α [Eq. (1)] is determined by the microstructure of the superconductor. For example, in Nb_3Sn this prefactor is inversely proportional to the grain size.[50] It is clear from Table I that α increases as the grain size increases. Nevertheless we consider this a very preliminary result, since it is unlikely that the grain size is the only microstructural feature that determines α. We are at present investigating in more detail the microstructural dependence of α.

D. The Fietz-Webb sclaing law

In order to extend the Fietz-Webb analysis to anisotropic superconductors it is necessary to meet two requirements. First, the analysis must be restricted to fields and temperatures where all the grains are superconducting. Unless this requirement is met, the active area over which current flows is no longer the cross-sectional area of the sample, but is instead a complicated (and in practice unmeasurable) function of field and temperature determined by which grains are superconducting and which grains are normal. The first requirement is met by considering single-crystal data. In La-Sr-Cu-O, single-crystal[36] data suggest that the reduction in J_{ct} we have observed at high fields occurs because for some orientations of the grains the applied field is above B_{c2}. In light of this, we have restricted our analysis to intermediate field levels. The second requirement is to determine an appropriate average value for B_{c2}. Since the formalism for calculating the appropriate value of B_{c2} to substitute into the Fietz-Webb scaling law for these anisotropic superconductors has not been developed, we have considered three different criteria for B_{c2}. It can be seen in Fig. 10 that regardless of which criterion is used for B_{c2}, the volume pinning force obeys the Fietz-Webb scaling law.

An additional complexity not found in the metallic superconductors, can be expected in these anisotropic superconductors. Since the fundamental parameters in La-Sr-Cu-O will vary considerably from grain to grain depending on their orientation, one can expect a very broad distribution in the pinning properties. This will lead to a broad E-J characteristic.[51,52] It has been demonstrated in Fig. 11 that the broad E-J characteristic is such that the scaling of J_{ct} is only weakly dependent on the electric field criterion in the range 2–20 μV cm^{-1}.

In order to assess the generality of the data obtained, two samples with different grain sizes have been measured. To within experimental error, both samples have the same functional form for the volume pinning force.

Most importantly since the functional form of the volume pinning force obeys the Fietz-Webb scaling law, this is very strong evidence indeed that flux pinning is the mechanism which determines $J_{ct}(B,T)$.

E. A qualitative model for flux pinning

In order to calculate the volume pinning force, the elastic constants of the flux-line lattice and the fundamental mechanisms which characterize the superconducting state in field-temperature space are a minimum requirement. These characteristic parameters have been calculated for isotropic nonparamagnetically limited superconductors.[53] Since the high-T_c oxides are not in this class, these calculations are not directly applicable to the La-Sr-Cu-O investigated here. For example, if we compare the volume pinning force of V_3Ga (Ref. 25) with that of $(Nb,Ta)_3Sn$,[27] in both cases F_p obeys the Fietz-Webb scaling law. However although grain boundary pinning operates in both materials, the field and temperature dependences of F_p in these two systems are quite different, $-F_p(V_3Ga)=\alpha B_{c2}^3(T)$ whereas $F_p((Nb,Ta)_3Sn)=\alpha B_{c2}^2(T)b^{1/2}(1-b)^2$. This difference in the functional form of F_p is attributed to paramagnetic limiting operating in V_3Ga but not in $(Nb,Ta)_3Sn$.[54,55] Until we can determine the role of microscopic mechanisms causing the superconductivity, it will not be possible to evaluate the details of the field and temperature dependence of the volume pinning force in high-T_c oxide superconductors.

There is a stark contrast between the critical current density of high-purity single crystals of metallic and oxide superconductors. In the metallic superconductors the critical current density in single crystals is close to zero. In comparison the critical current density of single crystals of high-T_c superconductors is very large indeed. This difference has profound implications for flux pinning. In polycrystalline metallic superconductors, one can expect the motion of flux across the grains themselves. However, in the oxide superconductors, flux motion across the grains is prevented by the pinning sites within the grains.

At the low values of pinning force measured here, since the large intragranular critical current densities suggest that flux does not cross the grains, the most important path for the flux to cross the sample is along the grain boundaries. Flux flow along grain boundaries is supported by some limited decoration measurements in $Y_1Ba_2Cu_3O_7$,[56] in which when no transport current is applied to the samples both the grain boundaries and the grains are decorated. However, when a transport current is applied the grains alone are decorated.[56] This is direct evidence for flux flow along grain boundaries.

A possible explanation for the low value of J_{ct} is that only a fraction of the entire cross-sectional area of the sample is active. This is the basis of the percolative model discussed in the Introduction.[15–17] Experimentally we measure an average intergranular volume pinning force. It is clear that in order for this average value to obey the scaling law, the active cross-sectional area over which current flows cannot be an arbitrary function of field and temperature. Hence we can consider two totally distinct regions in the sample, i.e., superconducting regions in which J_{ct} is determined by flux pinning, and those remaining grain boundaries which are totally impenetrable to superelectrons over the range of field and temperatures for which F_p obeys the scaling law. Alternatively we can make the simplest assumption, namely that the active area is the cross-sectional area of the sample. This is the assumption in low-T_c metallic superconductors and

must be considered the most plausible until the reason for, and nature of, the totally impenetrable barriers has been outlined.

VI. THE CHANGING NATURE OF THE DISSIPATIVE STATE IN OXIDE SUPERCONDUCTORS

There is ample experimental data in the literature demonstrating that high-T_c oxide samples can be prepared which show granular or S-N-S behavior.[57–60] This section discusses the significance of these observations in light of the data presented in this work.

A. Granularity and S-N-S behavior at high temperatures

The granularity of oxide samples was discovered very early in the development of the high-T_c oxides. Bednorz and Muller[59] and Wu *et al.*[60] found a strong depression of the zero-resistance state by applying very weak fields. Indeed, an exponential decrease of the critical current density with magnetic field has been found.[61,57] This suggests that close to T_c the superconducting path is maintained across normal junctions which have superconductivity induced in them because of weak proximity coupling. A similar low resistance tail has been observed in model system composites.[62] These composites consist of both superconducting and normal metal materials. The similarity between the resistive trace of these model systems and high-T_c systems provides evidence that this weak-field resistive tail is due to the suppression of weak proximity coupling.

In polycrystalline samples it is reasonable to expect a distribution in the fundamental parameters throughout the sample. Hence we can associate the S-N-S type behavior with normal regions or regions of lower critical temperature. It is not clear to what degree S-N-S-type properties are intrinsic, since the structure and chemistry of the grain boundaries are sensitive to the details of fabrication.[17,63] Indeed significant increases in the zero-resistance temperature in weak fields have been achieved by improving the preparation techniques.

B. Flux pinning at low temperatures

Extensive Auger spectroscopy[63] on similarly prepared samples of La-Sr-Cu-O has demonstrated that the equilibrium segregation of Sr to the grain boundaries results in a grain boundary composition that in a bulk form of the K_2NiF_4 structure, would indeed be superconducting.[64] Nevertheless, it is probable that the structure and chemistry of the grain boundary will cause a decrease in the fundamental superconducting parameters locally. Although this depression inevitably reduces the depairing current density (J_D) across the grain boundary compared to the bulk, the authors suggest that the depression in J_D at the grain boundaries in La-Sr-Cu-O is not the mechanism limiting J_{ct} at high fields. The scaling law we have found suggests that flux pinning is the mechanism which determines J_{ct} in high fields.

Degradation of the superconducting properties at the grain boundaries is found in the low-T_c superconductor NbN.[9] In NbN, although the grain boundaries are nonstoichiometric and their resistivity is much higher than the bulk, J_{ct} is not limited by poor coupling between the grains. In NbN, J_{ct} obeys the Kramer[29] dependence and is hence determined by flux pinning.

A prominent feature of the functional form of J_{ct} is its precipitous drop in very low fields (<0.05 T). A number of authors have suggested that the change in structure and chemistry at the grain boundaries is sufficiently gross that the proximity effect plays a dominant role.[15,16] It is of note that the highly field-dependent functional form of J_{ct} in very weak fields need not necessarily result from the suppression of this coupling between the grains but may be an intrinsic property of the flux pinning at the grain boundaries. For example, a mechanism that is used by Pippard[65] to explain the anomalous increase in J_{ct} close to $B_{c2}(T)$ (i.e., the peak effect) may operate. He suggests that when the rigidity of the flux line lattice falls to zero in the limit $b \rightarrow 1$, the flux-line lattice (F-L-L) conforms readily to the pinning structure. This interpretation suggests that a phase transition in the F-L-L, from a nonsynchronous F-L-L where the fluxon-fluxon interactions are important and not all the fluxons sit in pinning sites, to a F-L-L synchronous with the pinning sites, leads to the anomalous increase in J_{ct}. Since the F-L-L elastic constants also fall to zero in the limit $b \rightarrow 0$,[53] this phase transition in the flux-line lattice may also occur close to zero field.[66] Hence this mechanism allows the possibility that the high J_{ct} in very low fields is due to a matching between the fluxons and the pinning structure which does not occur in high magnetic fields. The crucial point is that the low field form of J_{ct} does not demand in and of itself, that normal barriers which play no role in transmitting superelectrons in high fields *must* be present. This conclusion is supported by the precipitous drop of J_{ct} in weak fields which has been observed in some low-J_c metallic superconductors.[67] We do not yet understand the intrinsic superconducting properties, the role of the proximity effect, or the pinning mechanism at the grain boundaries. This understanding is required to clarify the mechanism which determines J_{ct} in weak fields, and why the grain boundaries in oxide superconductors have such poor flux pinning properties in high fields.

The interpretation of the high-field dependence of J_{ct} at high temperatures and low temperatures presented here for La-Sr-Cu-O has the same essential features to that postulated in a previous publication on $R\,Ba_2Cu_3O_7$ samples.[6] At high temperatures the sample has isolated superconducting regions which are weakly coupled via the proximity effect through regions which are normal. This leads to the S-N-S-type behavior which causes the critical current density to drop to zero in high fields. However, at low temperatures, in good quality superconductors, essentially the entire sample including the grain boundaries can transmit superelectrons. The system can be characterized by S-S'-S, where S' represents the superconducting state found at the grain boundaries. In this low-temperature regime a field-independent J_{ct} is observed in high fields as we have found here for La-Sr-Cu-O and a flux pinning mechanism determines J_{ct}.

VII. FINAL COMMENTS

The volume pinning force has been characterized and found to be of the form

$$F_p = \alpha(D) B_{c2}^{2.4}(T) b \ .$$

The agreement between our data and a general Fietz-Webb universal scaling law is strong evidence that when the transport current density is defined at 10 μV cm^{-1}, a flux pinning mechanism determines J_{ct} in high fields. It is noted that in the original work demonstrating the significance of the scaling law by Fietz and Webb, they found that in the intermediate field range $F_p = \alpha B_{c2}^{2.5}(T) b$. To within experimental error, we have found the same field and temperature scaling dependence in this work.

It has been argued that although the superconducting properties may be degraded at the grain boundaries this is not the factor limiting J_{ct} in high fields. Rather, the present results indicate that it is the poor pinning properties of the grain boundaries in $La_{1.85}Sr_{0.15}CuO_4$ that cause the low J_{ct}. The authors suggest that the dissipative state is described by flux flow along the regions of weak flux pinning at the grain boundaries.

ACKNOWLEDGMENTS

The authors wish to thank in particular David C. Larbalestier with whom many interesting discussions were had in the course of preparing this manuscript. The authors also wish to acknowledge the help of the members of the Francis Bitter National Magnet Laboratory (Boston, MA), in particular B. Brandt and L. Rubin. We also acknowledge the support of U.S. Department of Energy Grant No. DE-FG02-87ER 45307 and an Office of Naval Research grant (for J.A.S.I.).

[1]P. Chaudhari, J. Mannhart, D. Dimos, C. C. Tsuei, J. Chi, M. Oprysko, and M. Scheuermann, Phys. Rev. Lett. **60**, 1653 (1988).

[2]D. Dimos, P. Chaudhari, J. Mannhart, and F. K. LeGoues, Phys. Rev. Lett. **61**, 219 (1988).

[3]J. S. Satchell, R. G. Humphreys, N. G. Chew, J. A. Edwards, and M. J. Kane, Nature **334**, 331 (1988).

[4]M. Suenaga, A. Ghosh, T. Asana, R. L. Sabatini, and A. R. Moodenbaugh, in *High Temperature Superconductors,* edited by D. U. Gubser and M. Schulter (Material Research Society, Pittsburgh, Pennsylvania, 1987), Vol. EA-11, p. 247.

[5]D. C. Larbalestier, M. Daeumling, X. Cai, J. Seuntjens, J. McKinnell, D. P. Hampshire, P. Lee, C. Meingast, T. Willis, H. Muller, R. D. Ray, R. G. Dillenburg, E. E. Hellstrom, and R. Joynt, J. Appl. Phys. **62**, 3308 (1987).

[6]D. P. Hampshire, X. Cai, J. Seuntjens, and D. C. Larbalestier, Super. Sci. Tech. **1**, 12 (1988).

[7]M. Daeumling, J. Seuntjens, and D. C. Larbalestier, Appl. Phys. Lett. **52**, 590 (1988).

[8]H. Kupfer, I. Apfelstedt, R. Flukiger, R. Meier-Hirmer, W. Schauer, T. Wolf, and H. Wuhl, Physica **153C**, 367 (1988).

[9]K. E. Gray, R. T. Kampwirth, J. M. Murduck, and D. W. Capone, II, Physica **152C**, 445 (1988).

[10]G. Deutscher, Physica **153C**, 15 (1988).

[11]G. Deutscher and K. A. Muller, Phys. Rev. Lett. **59**, 1745 (1987).

[12]J. Bardeen, L. N. Cooper, and J. R. Schreiffer, Phys. Rev. **108**, 1175 (1957).

[13]J. Bardeen, D. M. Ginsberg, and M. B. Salamon, in *Proceedings of the International Workshop on Novel Mechanisms of Superconductivity, Berkeley, California, 1987,* edited by S. A. Wolf and V. Z. Kresin (Plenum, New York, 1987).

[14]H. Kupfer, I. Apfelstedt, R. Flukiger, C. Keller, R. Meier-Hirmer, B. Runtsch, A. Turowski, U. Wiech, and T. Wolf, Cryogenics **28**, 650 (1988).

[15]R. L. Peterson and J. W. Ekin, Phys. Rev. B **37**, 9848 (1988).

[16]J. W. Ekin, J. Appl. Phys. **49**, 3406 (1978).

[17]D. C. Larbalestier, S. E. Babcock, X. Cai, M. Daeumling, D. P. Hampshire, T. F. Kelly, L. A. LaVanier, P. J. Lee, and J. Seuntjens, Physica **153-155C**, 1580 (1988).

[18]A. J. Panson, G. R. Wagner, A. I. Braginski, J. R. Gavaler, M. A. Jonocko, H. C. Pohl, and J. Talvacchio, Appl. Phys. Lett. **50**, 1104 (1987).

[19]M. Suzuki and T. Murakami, J. Appl. Phys. **29**, 1135 (1986).

[20]L. D. Cooley, M. Daeumling, T. C. Willis, and D. C. Larbalestier, IEEE Trans. Magn. **MAG-25**, 2314 (1989).

[21]D. P. Hampshire, J. Seuntjens, L. D. Cooley, and D. C. Larbalestier, Appl. Phys. Lett. **53**, 814 (1988).

[22]Y. M. Chiang, J. A. S. Ideda, and A. Roshko, in *Grain Boundary Segregation and Critical Current Density in $YBa_2Cu_3O_{7-x}$ Superconductors, Ceramic Superconductors II, Research Update 1988,* edited by M. F. Yan (The American Ceramic Society, Westerville, Ohio, 1988), pp. 607–618.

[23]J. Bardeen and M. J. Stephen, Phys. Rev. **149**, A1197 (1965).

[24]W. A. Fietz and W. W. Webb, Phys. Rev. **178**, 657 (1969).

[25]D. P. Hampshire, A. F. Clark, and H. Jones, J. Appl. Phys. **66**, 3160 (1989).

[26]B. Seeber, C. Rossel, O. Fischer, and W. Glaetze, IEEE Trans. Magn. **MAG-19**, 402 (1983).

[27]D. P. Hampshire, H. Jones, and E. W. J. Mitchell, IEEE Trans. Magn. **MAG-21**, 289 (1985).

[28]D. P. Hampshire and H. Jones, in *Proceedings of the Ninth International Conference on Magnet, Technology, Zurich, 1984,* edited by C. Marinucci (Swiss Institute for Nuclear Research, Zurich, 1985), p. 531.

[29]E. J. Kramer, J. Appl. Phys. **44**, 657 (1969).

[30]D. Dew-Hughes, Philos. Mag. **30**, 293 (1974).

[31]U. Essmann, H. Trauble, Phys. Lett. **24A**, 526 (1967).

[32]O. Singh, A. E. Curzon, and C. C. Koch, J. Phys. D **9**, 61 (1976).

[33]R. G. Hampshire and M. T. Taylor, J. Phys. F **2**, 89 (1977).

[34]W. Sweet, Phys. Today **47**, 61 (1988).

[35]A. Roshko, Y. M. Chiang, J. S. Moodera, and D. A. Rudman, in Ref. 22, pp. 308–314.

[36]Y. Hidaka, Y. Enomoto, M. Suzuki, M. Oda, and T. Murakami, J. Appl. Phys. **26**, L377 (1987).

[37]R. Renker, I. Apfelstedt, H. Kupfer, C. Politis, H. Rietschel, W. Schauer, H. Wuhl, U. Gottwick, H. Kneissel, U. Rauchschwalbe, H. Spille, and F. Steglich, Z. Phys. B **67**, 1 (1987).

[38]S. M. Johnson, M. T. Gusman, D. J. Rowcliffe, T. H. Geballe, and J. Z. Sun, Adv. Ceram. Mater. **2**, 337 (1987).
[39]J. W. Ekin, A. J. Panson, and B. A. Blankenship, in *High Temperature Superconductors,* Symposium Proceedings No. 99, edited by M. B. Brodsky, H. L. Tuller, R. C. Dynes, and K. Kitazawa (Materials Research Society, Pittsburgh, Pennsylvania 1988), p. 283.
[40]A. P. Malozemoff, T. K. Worthington, Y. Yeshurun, F. Holtzberg, and P. H. Kes, Phys. Rev. B **38**, 7203 (1988).
[41]L. Krusin-Elbaum, A. P. Malozemoff, Y. Yeshurun, D. C. Cronemeyer, and F. Holtzberg, Physica **153C**, 1469 (1988).
[42]T. P. Orlando, E. J. McNiff, S. Foner, and M. R. Beasley, Phys. Rev. B **19**, 4545 (1979).
[43]M. Suenaga and D. O. Welch, in *Filamentary AIS Superconductors, Cryogenic Material Series,* edited by M. Suenaga and A. F. Clark (Plenum, New York, 1980), p. 131.
[44]Y. Yeshurun and A. P. Malozemoff, Phys. Rev. Lett. **60**, 2202 (1988).
[45]M. Tinkham, Phys. Rev. Lett. **13**, 804 (1964).
[46]Y. B. Kim, C. F. Hempstead, and C. F. Strand, Phys. Rev. **139**, A1163 (1965).
[47]S. J. Poon and K. M. Wong, Phys. Rev. B **27**, 6985 (1983).
[48]L. P. Gorkov and N. B. Kopnin, Zh. Eksp. Teor. Fiz. **64**, 356 [Sov. Phys—JETP **37**, 183 (1973)].
[49]D. P. Hampshire and H. Jones, J. Phys. C **20**, 3533 (1987).
[50]W. Schauer and W. Schelb, IEEE Trans. Magn. **MAG-17**, 374 (1981).
[51]D. P. Hampshire and H. Jones, Cryogenics **27**, 608 (1987).
[52]W. H. Warnes and D. C. Larbalestier, Cryogenics **26**, 643 (1986).
[53]E. H. Brandt, J. Low Temp. Phys. **26**, 709 (1977).
[54]N. R. Werthamer, E. Helfand, and P. C. Hohenberg, Phys. Rev. **147**, 295 (1966).
[55]D. Dew-Hughes, Cryogenics **15**, 435 (1975).
[56]A. Ourmazd, J. A. Rentschler, W. J. Skocpol, and D. W. Johnson, Phys. Rev. B **36**, 8914 (1987).
[57]P. England, T. Venkatesan, X. D. Wu, A. Inam, M. S. Hegde, T. L. Cheeks, and H. G. Craighead, Appl. Phys. Lett. **53**, 2336 (1988).
[58]D. K. Finnemore, J. E. Ostenson, L. Ji, R. W. McCallum, and J. R. Clem, Adv. Cryo. Eng. **34**, 613 (1988).
[59]J. B. Bednorz and K. A. Muller, Z. Phys. B **64**, 189 (1986).
[60]M. K. Wu, J. R. Ashburn, C. J. Torng, P. H. Hor, R. L. Meng, L. Gau, Z. J. Huang, Y. Q. Wang, and C. W. Chu, Phys. Rev. Lett. **56**, 908 (1987).
[61]C. J. Jou, E. R. Weber, J. Washburn, and W. A. Soffa, Appl. Phys. Lett. **52**, 326 (1988).
[62]C. J. Lobb, M. Tinkham, and W. J. Skocpol, Solid State Commun. **27**, 1273 (1978).
[63]A. Roshko and Y.-M. Chiang (unpublished).
[64]Y. M. Chiang, A. Roshko, B. D. Fabes, D. K. Leung, J. A. S. Ikeda, D. A. Rudman, M. J. Parker, and J. R. Martin, Mat. Res. Soc. Symp. **99**, 821 (1988).
[65]A. B. Pippard, Philos. Mag. **19**, 217 (1968).
[66]D. P. Hampshire, J. V. A. Somerkoski, J. Cosier, and H. Jones, *Advances in Cryogenic Engineering,* (Plenum, New York, 1987), Vol. 34, p. 717.
[67]D. M. Kroeger, Solid State Commun. **7**, 843 (1969).

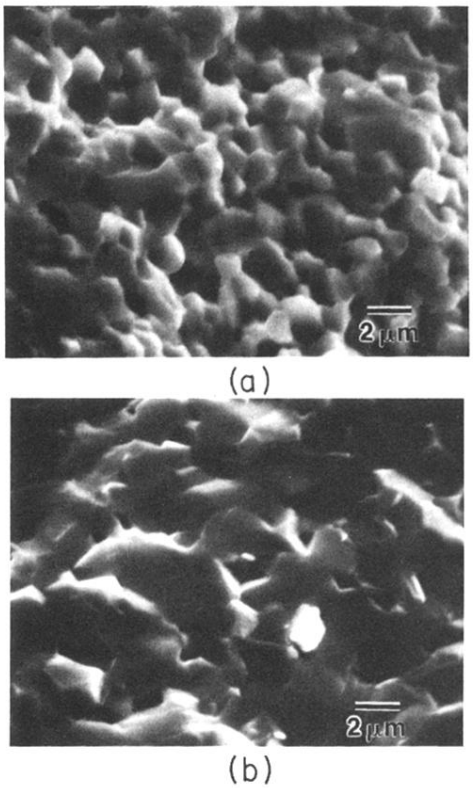

FIG. 1. Secondary electron images of the samples used in this work. (a) ~ 1 μm grain size (sample A); (b) ~ 3 μm grain size (sample B).